NASA TM X-53

NASA TM X-53

N63-12952
Code-1

TECHNICAL MEMORANDUM
X - 53

EXPERIMENTAL AND CALCULATED RESULTS OF A FLUTTER INVESTIGATION OF SOME VERY LOW ASPECT-RATIO FLAT-PLATE SURFACES AT MACH NUMBERS FROM 0.62 TO 3.00

By Perry W. Hanson and Gilbert M. Levey

Langley Research Center
Langley Field, Va.

Declassified February 6, 1962

NATIONAL AERONAUTICS AND SPACE ADMINISTRATION
WASHINGTON August 1959

copy

Code 1

1W

NATIONAL AERONAUTICS AND SPACE ADMINISTRATION

TECHNICAL MEMORANDUM X-53

EXPERIMENTAL AND CALCULATED RESULTS OF A FLUTTER INVESTIGATION OF SOME VERY LOW ASPECT-RATIO FLAT-PLATE SURFACES AT MACH NUMBERS FROM 0.62 TO 3.00

L
2
3
6

By Perry W. Hanson and Gilbert M. Levey

SUMMARY

Some very low aspect-ratio flat-plate surfaces of aluminum alloy were tested for flutter at Mach numbers from 0.62 to 3.00. Two types of plan forms, a delta and a delta with one-third span cut off, are used in this investigation. Three different panel aspect ratios, 0.728, 0.536, and 0.353, were tested for each type of plan form. Each model had a 12-inch root chord and was cantilevered from the tunnel wall.

Generally, the clipped-tip-delta plan forms were more susceptible to flutter throughout the Mach number range investigated. The lower aspect-ratio models fluttered at a higher value of the stiffness-altitude parameter than the higher aspect-ratio models for a given type of plan form and a given Mach number.

Modal-type calculations were made for some supersonic cases by using first-order piston-theory aerodynamic forces. Generally, the theoretical flutter boundaries agreed with the experimental boundaries within 20 percent. The theory was unconservative for the delta plan forms and conservative for the clipped-tip-delta plan forms.

INTRODUCTION

The use of very low aspect-ratio surfaces is becoming increasingly prevalent in the design of missile and rocket fins, supersonic aircraft, and hypersonic gliders. Although some work has been done in this area of interest (see, for example, refs. 1 to 3), data available for the flutter characteristics of these types of surfaces at both subsonic and supersonic speeds are meager. It is evident that there is a need for more information of this kind, both to provide trend data for design criteria and to provide a basis for comparison of theory and experiment. Therefore, a systematic investigation was made of the flutter characteristics of some configurations that might be considered representative of those found on these new vehicles.

Some flat-plate semispan models of two different types of plan forms, each with three different panel aspect ratios were tested at Mach numbers
from 0.62 to 3.00. The experimental results were compared with theo- L
retical calculations in the supersonic regime with the use of the method 2
of reference 4 based on the "piston theory" of reference 5. Mode shapes 3
of the models used in the computations were determined by the method of 6
reference 6.

SYMBOLS

A	panel aspect ratio (Semispan^2/Panel area)
a	velocity of sound, ft/sec
b	semichord at 3/4 semispan, in.
$\frac{b\omega_\alpha}{a}\sqrt{\mu}$	stiffness-altitude parameter
c	local chord, in.
f_f	flutter frequency, cps
f_n	natural frequency of nth mode (n = 1, 2, 3, and 4), cps
l	length of semispan of model, measured normal to stream direction, in.
M	Mach number
q	dynamic pressure, lb/sq ft
t	thickness, in.
W	total weight of surface, lb

x chordwise station, measured parallel to root chord from leading edge, in.

y spanwise station, measured perpendicular to root chord from the root

δ leading- and trailing-edge bevel, measured perpendicular to edges, in.

μ mass density parameter

L236

ρ air density, slugs/cu ft

ω_α wing torsional circular frequency, radians/sec

Subscripts:

ex experimental

th theoretical

MODEL DESCRIPTION

The six model configurations used in the investigation are shown in figure 1. They consisted of two types of plan forms: delta and delta with the outer one-third span cut off. The three delta plan forms were 70°, 75°, and 80° deltas with corresponding panel aspect ratios of 0.728, 0.536, and 0.353 for 12-inch root chords. The three clipped-tip-delta plan forms also had 12-inch root chords, and the dimensions of these plan forms were chosen to give the same aspect ratios as the delta plan forms.

All the models were made from 2024-T3 aluminum-alloy sheets with the thicknesses and leading- and trailing-edge bevels as indicated in figure 1. The models were mounted in the wind-tunnel side wall and clamped between two 1/2-inch-thick steel plates over the entire root chord. These plates were made to hold the models 1/2 inch out from the wind-tunnel wall in a triangular shaped body. The method of mounting is illustrated in figure 2.

TEST PROCEDURE

The tests were conducted in the Langley 9- by 18-inch supersonic aëroelasticity tunnel. This tunnel is of the intermittent blowdown type with fixed nozzle blocks and operates from a high-pressure source to a vacuum. The transonic tests of the delta plan forms were made with the use of a slotted-test-section nozzle with a choking device employed in the diffuser to obtain the desired Mach number in the test section.

The tests were made at constant Mach number with the dynamic pressure being increased until flutter was encountered or until the tunnel limits were reached. During each test, continuous records of wind-tunnel conditions and model behavior were recorded on an oscillograph.

Generally, the models were not damaged during flutter tests and could be used for succeeding tests. When models were damaged and new ones were made, it was found that the models could be duplicated very easily and that the natural frequencies and node lines of the new models were virtually the same as those of the previous models. The variations in natural frequencies listed in table I were probably the result of small differences in tightness of the root mount. Resistance wire strain-gage bridges mounted at the root of the model at about 70 percent of the chord were used to record natural frequencies listed in table I. Mode shapes of the models were obtained by the method of reference 6 for use in the piston-theory analysis and are presented in table II along with typical natural vibration node lines of the first four modes.

RESULTS AND DISCUSSION

The experimental and theoretical results are listed in table I and are shown in figure 3 in which both an experimental and a theoretical stiffness-altitude parameter $\frac{b\omega_\alpha}{a}\sqrt{\mu}$ required for flutter are plotted as a function of Mach number. The ω_α is the second natural frequency f_2 which is predominantly torsional for all models. The mass-density parameter μ is the ratio of the mass of the wing to the mass of a volume of air enclosing the wing. For the delta plan forms, the volume is that of a cone with the base diameter parallel to the airstream and equal to the root chord. For the clipped-tip-delta plan forms, the volume is that of a truncated cone with the two ends parallel to the airstream with diameters equal to the root and tip chords. The air density ρ, which is used in the computation of μ, is the test-section density at flutter. In figure 3 constant-density (altitude) lines are horizontal and density decreases as $\frac{b\omega_\alpha}{a}\sqrt{\mu}$ increases. Constant dynamic pressure lines are radial from the origin and increase clockwise. The flutter region is below the curves and the no-flutter region is above the curves.

When figures 3(a), 3(b), and 3(c) are compared, several general observations can be made. The flutter boundaries for the delta-plan-form models showed little change with aspect ratio except for the lowest aspect-ratio model at the higher Mach numbers. The clipped-tip-delta-plan-form models, however, exhibited a considerable change in the flutter boundaries with aspect ratio. (See figs. 3(d), 3(e), and 3(f).) As the aspect ratio decreased, the flutter boundary was raised. For a given aspect ratio, the clipped-tip-delta plan forms fluttered at a higher value of the stiffness-altitude parameter than the deltas at all Mach numbers.

The theoretical flutter boundaries shown in figure 3 were calculated with the use of aerodynamic forces obtained from first-order piston theory and using the first three (experimentally determined) natural-vibration modes. When the theoretical and experimental flutter boundaries are compared, it is seen that the shape of the boundaries agrees very well for all the cases considered except for the lowest aspect-ratio delta (fig. 3(c)). The agreement between the experimental and theoretical flutter boundaries is poor at all Mach numbers for the lowest aspect-ratio model of the clipped-tip-delta models. Generally, the theoretical flutter boundaries were conservative with respect to the experimental boundaries for the clipped-tip-delta plan forms; that is, a greater density was required to flutter the models than was predicted by theory. For the delta plan forms, however, the theory was unconservative.

Figure 4 shows the variation of the ratio of theoretical flutter frequency to experimental flutter frequency with Mach number. In all cases, the theoretical flutter frequency was greater than the experimental flutter frequency. For the delta-plan-form models, the agreement between the theoretical and experimental flutter frequencies was best for the largest aspect-ratio model and became worse as the aspect ratio decreased, whereas the opposite was true for the clipped-tip-delta-plan-form models.

CONCLUDING REMARKS

An investigation conducted in the Langley 9- by 18-inch supersonic aeroelasticity tunnel of very low aspect-ratio flat-plate models with two types of plan forms and three aspect ratios for each type of plan form indicate that the clipped-tip-delta plan forms were more susceptible to flutter than the delta plan forms throughout the Mach number range investigated. For a given Mach number and a given type of plan form, the lower aspect-ratio models fluttered at a higher value of the stiffness-altitude parameter than the higher aspect-ratio models. The agreement between the experimental flutter boundaries and the theoretical flutter boundaries (as computed from first-order piston theory) was generally good. The theory was conservative for the clipped-tip deltas and unconservative for the deltas. The agreement was poorest for the lowest aspect-ratio models of both types of plan forms.

Langley Research Center,
National Aeronautics and Space Administration,
Langley Field, Va., May 12, 1959.

L
2
3
6

REFERENCES

1. Jones, George W., Jr., and Young, Lou S., Jr.: Transonic Flutter Investigation of Two 64° Delta Wings With Simulated Streamwise Rib and Orthogonal Spar Construction. NACA RM L56I27, 1957.

2. Jones, George W., Jr.: Transonic Flutter Investigation of a 64° Delta Wing Constructed With Spars Along Constant-Percent Chord Lines and Streamwise Ribs. NACA RM L57G01, 1957.

3. Fralich, Robert W., Hedgepeth, John M., and Tuovila, W. J.: Flutter and Divergence of Rectangular Wings of Very Low Aspect Ratio. NACA RM L57F24, 1957.

4. Morgan, Homer G., Huckel, Vera, and Runyan, Harry L.: Procedure for Calculating Flutter at High Supersonic Speeds Including Camber Deflections, and Comparison With Experimental Results. NACA TN 4335, 1958.

5. Ashley, Holt, and Zartarian, Garabed: Piston Theory - A New Aerodynamic Tool for the Aeroelastician. Jour. Aero. Sci., vol. 23, no. 12, Dec. 1956, pp. 1109-1118.

6. Hanson, Perry W., and Tuovila, W. J.: Experimentally Determined Natural Vibration Modes of Some Cantilever-Wing Flutter Models by Using an Acceleration Method. NACA TN 4010, 1957.

TABLE I.- EXPERIMENTAL AND THEORETICAL RESULTS

Frequencies, cps					M	Flutter conditions				$\frac{b\omega_\alpha}{a}\sqrt{\mu}$		$\frac{f_{f,th}}{f_{f,ex}}$
f_1	f_2	f_3	f_4	$f_{f,ex}$		ρ, slug/cu ft	a, fps	q, lb/sq ft	μ	Exp.	Theory	
Model 1A												
78	183	325	395	166	0.63	0.001505	1,102	363	17.17	0.54	----	----
72	171	320	367	150	.64	.001442	1,093	354	17.93	.52	----	----
78	186	320	398	157	.75	.001307	1,089	436	19.80	.60	----	----
79	193	350	396	150	.79	.001471	1,077	532	17.58	.59	----	----
78	186	322	398	140	.88	.001346	1,070	598	19.20	.60	----	----
79	186	331	398	140	.96	.001281	1,051	652	20.18	.63	----	----
79	192	350	402	142	.96	.001339	1,053	685	19.30	.63	----	----
78	178	342	388	148	1.01	.001006	1,039	555	25.67	.68	----	----
77	181	320	367	133	1.19	.000760	1,013	553	34.00	.82	----	----
75	170	305	367	150	1.30	.000786	980	643	32.98	.78	0.62	1.15
76	173	318	372	160	1.64	.000736	915	829	35.12	.88	.72	1.07
75	173	320	379	153	2.00	.000592	850	846	43.67	1.06	.79	1.12
76	173	320	375	160	2.55	.000651	770	1,264	39.70	1.11	.90	1.08
75	174	325	383	161	3.00	.000736	721	1,723	35.10	1.12	.98	1.06
Model 1B												
127	277	457	640	222	0.62	0.003993	1,107	943	6.34	0.50	----	----
127	275	457	627	225	.75	.003213	1,086	1,065	7.88	.56	----	----
128	277	460	642	214	.86	.002666	1,071	1,130	9.50	.63	----	----
129	275	467	646	210	1.14	.002404	1,024	1,641	10.54	.69	0.53	1.79
128	273	460	644	264	1.25	.002570	1,012	2,058	9.86	.67	.57	1.39
126	271	458	635	245	1.26	.002364	1,007	1,906	10.71	.69	.57	1.50
127	275	457	640	250	1.30	.002380	988	1,963	10.64	.71	.60	1.49
130	283	462	650	300	1.64	.002453	949	2,915	10.32	.76	.70	1.26
123	267	454	600	238	2.00	.001510	870	2,278	16.36	.99	.84	1.18
127	269	460	600	250	2.55	.001210	796	2,490	13.96	.99	.78	1.09
125	273	450	625	(a)	3.00	[a].001017	[a]731	[a]2,448	24.90	1.47	.85	----
Model 1C												
213	386	580	738	314	0.63	0.004195	1,109	1,025	5.16	0.62	----	----
217	383	575	750	316	.75	.003132	1,086	1,038	6.91	.73	----	----
215	389	580	744	300	.90	.002911	1,066	1,340	7.43	.78	----	----
212	387	580	738	306	1.16	.002401	1,020	1,681	9.01	.90	0.85	1.72
213	375	567	720	300	1.24	.002188	997	1,675	9.89	.93	.89	1.74
217	388	554	725	350	1.30	.002488	990	2,058	8.70	.91	.99	1.45
216	400	585	775	360	1.64	.002104	928	2,435	10.27	1.09	1.08	1.48
210	467	560	786	313	2.00	.001468	859	2,092	15.25	1.31	1.11	1.61
213	400	600	833	300	3.00	.000948	748	2,392	22.82	2.00	1.42	1.81
Model 2A												
35	95	183	209	93	1.30	0.000628	979	509	38.67	0.95	0.97	1.75
35	100	188	208	102	1.64	.000581	918	660	41.79	1.11	1.18	1.64
36	105	197	233	94	2.00	.000724	847	1,039	33.55	1.13	1.20	1.88
35	110	196	232	100	2.55	.000799	777	1,580	30.40	1.23	1.43	1.76
34	109	193	233	105	3.00	.000655	720	1,533	37.08	1.45	1.57	1.86
Model 2B												
60	122	225	325	115	1.30	0.000618	977	498	39.32	1.24	1.36	1.70
59	114	213	331	108	1.64	.000397	916	449	61.18	1.53	1.50	1.71
60	125	229	332	117	2.00	.000495	847	710	49.11	1.63	1.71	1.70
59	117	207	318	109	3.00	.000363	693	784	66.97	2.18	2.21	1.66
Model 2C												
126	216	350	507	175	1.30	0.001305	982	1,062	18.61	1.49	2.24	1.21
125	213	358	500	183	1.64	.001120	924	1,286	21.69	1.69	2.55	1.13
122	204	342	487	165	2.00	.000754	858	1,110	32.18	2.12	2.87	1.20
130	218	368	540	183	2.55	.000829	790	1,677	29.30	2.34	3.18	1.14
118	197	323	485	170	3.00	.000642	714	1,472	37.81	2.67	3.51	1.12

[a]No flutter - maximum tunnel conditions.

TABLE II.- REPRESENTATIVE MODE SHAPES AND NODE LINES OF MODELS

[Deflections normalized on maximum deflection, considered positive when deflected wing is above static position]

(a) Model 1A

x/c	Normalized deflection at y/l =									
	0.10	0.20	0.30	0.40	0.50	0.60	0.70	0.80	0.90	1.00
f_1 = 76 cps										
0	0.004	0.012	0.019	0.033	0.060	0.130	0.331	0.550	0.775	1.000
.25	.009	.018	.033	.062	.124	.275	.443	.625	.810	1.000
.50	.014	.034	.061	.120	.233	.363	.514	.670	.830	1.000
.75	.023	.082	.152	.235	.353	.465	.587	.715	.850	1.000
1.00	.058	.131	.216	.306	.418	.525	.639	.750	.875	1.000
f_2 = 165 cps										
0	-0.019	-0.045	-0.116	-0.345	-0.719	-0.900	-0.836	-0.415	0.190	1.000
.25	-.042	-.135	-.348	-.600	-.741	-.800	-.676	-.255	.330	1.000
.50	-.100	-.225	-.443	-.560	-.555	-.600	-.353	.100	.550	1.000
.75	-.023	-.060	-.124	-.160	-.084	.115	.321	.550	.770	1.000
1.00	.096	.310	.487	.590	.683	.745	.815	.875	.935	1.000
f_3 = 291 cps										
0	-0.024	-0.170	-0.533	-0.780	-0.783	-0.592	1.000	1.000	0.294	-0.864
.25	-.155	-.400	-.729	-.745	-.352	.553	1.000	.990	.095	-.864
.50	-.209	-.230	-.108	.150	.486	.587	.525	.380	-.466	-.864
.75	.105	.190	.280	.360	.416	.256	-.228	-.500	-.722	-.864
1.00	-.256	-.600	-.844	-.930	-.950	-.938	-.850	-.710	-.729	-.864
f_4 = 383 cps										
0	0.007	0.030	0.062	0.130	0.117	-0.050	0.060	0.360	0.940	1.000
.25	.032	.060	.071	.035	-.038	-.025	.109	.380	.771	1.000
.50	-.007	-.020	-.037	-.040	-.044	-.045	.111	.380	.677	1.000
.75	-.034	-.075	-.111	-.150	-.161	-.150	.060	.340	.618	1.000
1.00	-.052	-.315	-.860	-.930	-.909	-.800	-.538	.250	.600	1.000

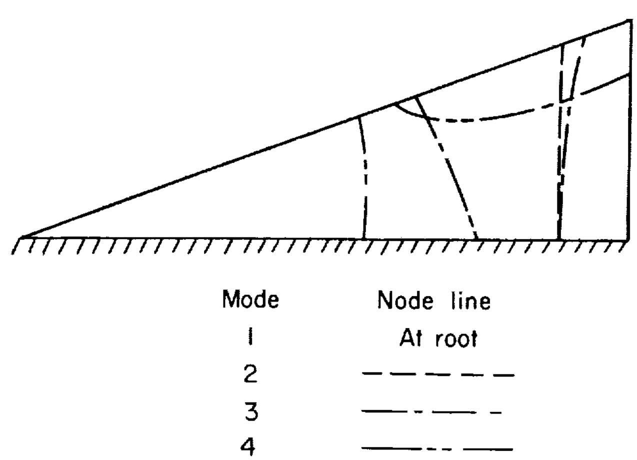

L-236

TABLE II.- REPRESENTATIVE MODE SHAPES AND NODE LINES OF MODELS - Continued

(b) Model 1B

x/c	Normalized deflection at y/l =									
	0.10	0.20	0.30	0.40	0.50	0.60	0.70	0.80	0.90	1.00
					f_1 = 124 cps					
0	0.001	0.002	0.007	0.015	0.034	0.095	0.200	0.327	0.561	1.000
.25	.001	.004	.013	.028	.078	.159	.267	.389	.615	1.000
.50	.004	.016	.041	.089	.162	.244	.348	.481	.684	1.000
.75	.013	.045	.103	.171	.250	.343	.456	.582	.743	1.000
1.00	.030	.085	.152	.223	.305	.401	.512	.624	.757	1.000
					f_2 = 278 cps					
0	0.002	0.012	0.043	0.132	0.330	0.754	1.000	0.633	-0.022	-0.968
.25	.011	.045	.139	.274	.553	.877	.598	.231	-.242	-.968
.50	.044	.135	.280	.382	.404	.352	.193	-.058	-.417	-.968
.75	.046	.099	.118	.104	.060	-.037	-.181	-.378	-.630	-.968
1.00	-.072	-.153	-.239	-.331	-.432	-.533	-.643	-.747	-.857	-.968
					f_3 = 457 cps					
0	0.014	0.068	0.291	0.709	1.000	0.926	-0.058	-0.560	-0.311	0.719
.25	.058	.254	.612	.813	.512	.038	-.532	-.544	.053	.719
.50	.141	.214	.211	.128	-.270	-.515	-.536	-.262	.302	.719
.75	-.031	-.183	-.250	-.270	-.237	-.119	.066	.271	.500	.719
1.00	.166	.304	.387	.454	.515	.572	.572	.658	.692	.719
					f_4 = 630 cps					
0	-0.007	-0.052	-0.562	-0.708	-0.458	0.225	0.472	-0.406	-0.815	-0.524
.25	-.180	-.340	-.319	-.140	.320	.412	-.108	-.680	-.729	-.524
.50	-.005	.036	.164	.166	.131	-.044	-.342	-.539	-.585	-.524
.75	.029	.088	.123	.133	.130	.100	-.064	-.195	-.385	-.524
1.00	.288	.791	.974	1.000	.954	.791	.495	.171	-.216	-.524

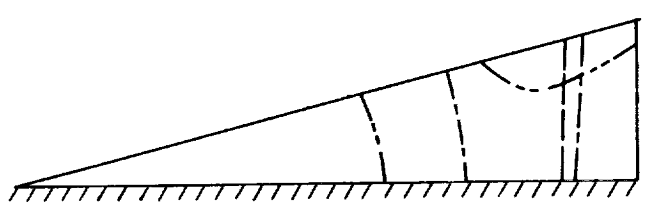

Mode	Node line
1	At root
2	- - - - -
3	—- - —- -
4	—- - - —- - -

TABLE II.- REPRESENTATIVE MODE SHAPES AND NODE LINES OF MODELS - Continued

(c) Model 1C

x/c	Normalized deflection at y/l =									
	0.10	0.20	0.30	0.40	0.50	0.60	0.70	0.80	0.90	1.00
f_1 = 242 cps										
0	0.003	0.006	0.012	0.019	0.029	0.047	0.135	0.365	0.635	1.000
.25	.004	.010	.017	.029	.047	.117	.295	.505	.700	1.000
.50	.006	.017	.032	.065	.135	.282	.425	.585	.760	1.000
.75	.010	.050	.117	.220	.320	.435	.545	.675	.820	1.000
1.00	.034	.084	.167	.286	.400	.524	.636	.757	.873	1.000
f_2 = 440 cps										
0	0.002	0.009	0.013	0.036	0.142	0.463	0.894	0.768	-0.005	-1.000
.25	.005	.018	.048	.169	.412	.753	.756	.458	-.320	-1.000
.50	.017	.077	.212	.379	.474	.505	.323	-.045	-.548	-1.000
.75	.050	.112	.133	.130	.080	-.021	-.198	-.507	-.759	-1.000
1.00	-.082	-.236	-.370	-.479	-.605	-.699	-.791	-.871	-.932	-1.000
f_3 = 650 cps										
0	0.009	0.018	0.039	0.079	0.373	0.608	0.374	-0.610	-0.472	1.000
.25	.015	.047	.125	.465	.499	.265	-.257	-.727	-.109	1.000
.50	.078	.242	.255	.169	-.041	-.370	-.618	-.434	.183	1.000
.75	-.027	-.077	-.178	-.269	-.373	-.293	-.066	.214	.512	1.000
1.00	.055	.154	.265	.378	.499	.612	.727	.835	.906	1.000

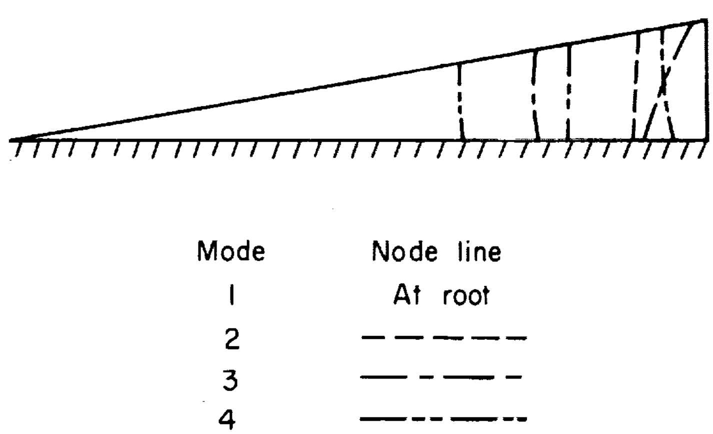

L-236

L-236

TABLE II.- REPRESENTATIVE MODE SHAPES AND NODE LINES OF MODELS - Continued

(d) Model 2A

x/c	Normalized deflection at y/l =									
	0.10	0.20	0.30	0.40	0.50	0.60	0.70	0.80	0.90	1.00
					f_1 = 36 cps					
0	0.013	0.032	0.064	0.125	0.215	0.310	0.404	0.515	0.657	0.904
.25	.018	.050	.097	.162	.261	.350	.457	.575	.741	.955
.50	.027	.068	.130	.200	.301	.392	.508	.630	.790	.973
.75	.039	.095	.171	.256	.358	.462	.569	.680	.814	.994
1.00	.046	.123	.217	.315	.428	.520	.611	.720	.837	1.000
					f_2 = 96 cps					
0	-0.031	-0.115	-0.226	-0.550	-0.785	-0.800	-0.757	-0.700	-0.636	-0.556
.25	-.073	-.250	-.495	-.620	-.664	-.660	-.636	-.550	-.432	-.138
.50	-.062	-.180	-.331	-.380	-.367	-.300	-.191	.040	.274	.547
.75	-.006	-.010	.017	.060	.135	.400	.386	.565	.710	.790
1.00	.080	.200	.380	.580	.772	.915	.916	.950	.982	1.000
					f_3 = 188 cps					
0	-0.042	-0.135	-0.266	-0.410	-0.491	-0.430	-0.222	0.300	0.715	1.000
.25	-.114	-.210	-.301	-.330	-.291	-.130	.127	.370	.635	.900
.50	-.073	-.170	-.251	-.280	-.223	-.060	.161	.410	.620	.830
.75	-.085	-.200	-.314	-.410	-.458	-.440	-.337	0	.330	.670
1.00	-.169	-.400	-.641	-.710	-.709	-.690	-.642	-.530	-.218	.450
					f_f = 204 cps					
0	0.055	0.220	0.424	0.530	0.557	0.520	0.268	0.100	0.069	0.118
.25	.087	.250	.320	.290	.151	-.040	-.131	-.150	-.125	.158
.50	-.049	-.100	-.161	-.270	-.388	-.410	-.371	-.190	.043	.279
.75	-.079	-.200	-.342	-.410	-.410	-.350	-.235	0	.284	.442
1.00	-.120	-.200	-.271	-.270	-.199	0	.327	.570	.789	1.000

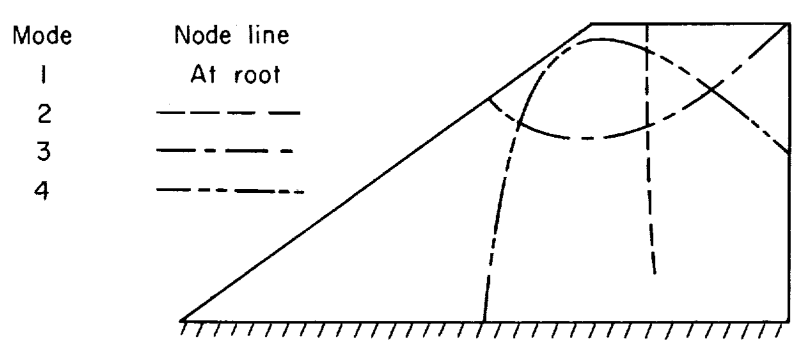

TABLE II.- REPRESENTATIVE MODE SHAPES AND NODE LINES OF MODELS - Continued

(e) Model 2B

x/c	Normalized deflection at y/l =									
	0.10	0.20	0.30	0.40	0.50	0.60	0.70	0.80	0.90	1.00
					f_1 = 60 cps					
0	0.005	0.018	0.039	0.069	0.114	0.177	0.277	0.407	0.572	0.730
.25	.009	.032	.068	.116	.185	.270	.384	.510	.678	.833
.50	.014	.048	.094	.156	.236	.347	.474	.602	.750	.904
.75	.028	.058	.144	.223	.317	.424	.553	.680	.823	.960
1.00	.037	.097	.169	.266	.368	.479	.608	.729	.867	1.000
					f_2 = 123 cps					
0	-0.010	-0.034	-0.074	-0.164	-0.320	-0.473	-0.506	-0.513	-0.491	-0.432
.25	-.024	-.079	-.161	-.290	-.385	-.420	-.417	-.387	-.318	-.156
.50	-.016	-.060	-.122	-.192	-.223	-.208	-.158	-.067	.067	.223
.75	-.007	-.009	.004	.043	.095	.168	.253	.351	.461	.586
1.00	.049	.149	.250	.348	.458	.565	.674	.784	.897	1.000
					f_3 = 222 cps					
0	0.077	0.261	0.756	0.935	0.990	1.000	0.973	0.854	-0.735	-0.919
.25	.397	.752	.812	.827	.808	.727	-.349	-.814	-.950	-.981
.50	.029	.058	.052	-.167	-.449	-.685	-.804	-.858	-.885	-.881
.75	-.157	-.213	-.236	-.244	-.244	-.244	-.244	-.244	-.244	-.244
1.00	.365	.187	.831	.908	.948	.969	.973	.960	.939	.904

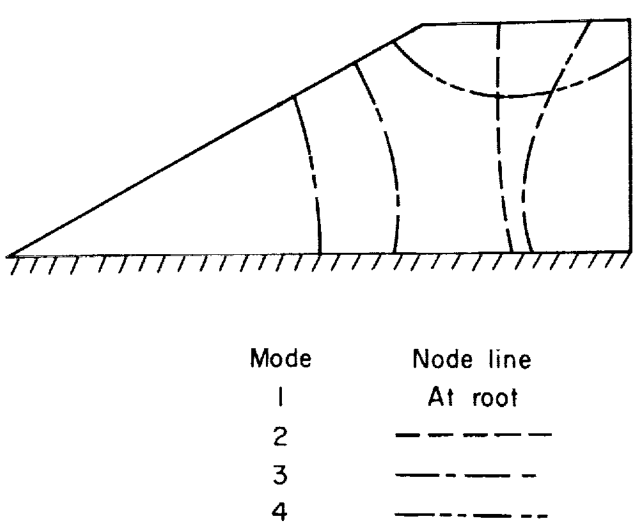

L-236

L-236

TABLE II.- REPRESENTATIVE MODE SHAPES AND NODE LINES OF MODELS - Concluded

(f) Model 2C

x/c	Normalized deflection at y/l =									
	0.10	0.20	0.30	0.40	0.50	0.60	0.70	0.80	0.90	1.00
	f_1 = 122 cps									
0	0.003	0.010	0.019	0.032	0.048	0.080	0.122	0.199	0.324	0.487
.25	.006	.016	.029	.054	.093	.144	.215	.324	.455	.599
.50	.010	.032	.061	.099	.157	.234	.330	.449	.593	.737
.75	.029	.067	.115	.179	.253	.356	.462	.587	.728	.875
1.00	.035	.093	.163	.247	.337	.439	.551	.696	.849	1.000
	f_2 = 214 cps									
0	0.006	0.020	0.060	0.123	0.210	0.375	0.702	0.875	0.954	1.000
.25	.032	.092	.167	.268	.403	.705	.787	.792	.772	.716
.50	.053	.056	.243	.324	.404	.450	.432	.307	.115	-.182
.75	.003	.008	.005	-.022	-.070	-.140	-.233	-.375	-.565	-.770
1.00	-.049	-.132	-.222	-.332	-.487	-.653	-.760	-.850	-.929	-1.000
	f_3 = 343 cps									
0	0.006	0.039	0.130	0.461	0.729	0.850	0.851	0.808	0.385	-0.515
.25	.158	.380	.531	.634	.702	.708	.475	-.278	-.617	-.818
.50	.030	.108	.115	.056	-.163	-.410	-.567	-.647	-.669	-.568
.75	-.061	-.141	-.224	-.261	-.252	-.199	-.129	-.020	.168	.416
1.00	.098	.250	.429	.592	.714	.807	.872	.926	.966	1.000
	f_4 = 518 cps									
0	-0.017	-0.054	-0.153	-0.453	-0.629	-0.695	-0.330	0.429	0.650	0.601
.25	-.165	-.274	-.300	-.246	-.067	-.300	.478	.472	-.049	-.455
.50	.009	.081	.136	.149	.137	.084	-.217	-.398	-.562	-.707
.75	-.024	-.071	-.130	-.191	-.252	-.306	-.319	-.290	-.219	-.118
1.00	.099	.303	.453	.586	.693	.785	.856	.915	.967	1.000

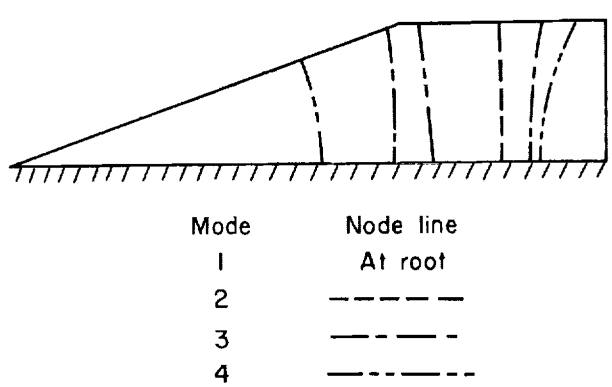

L-236

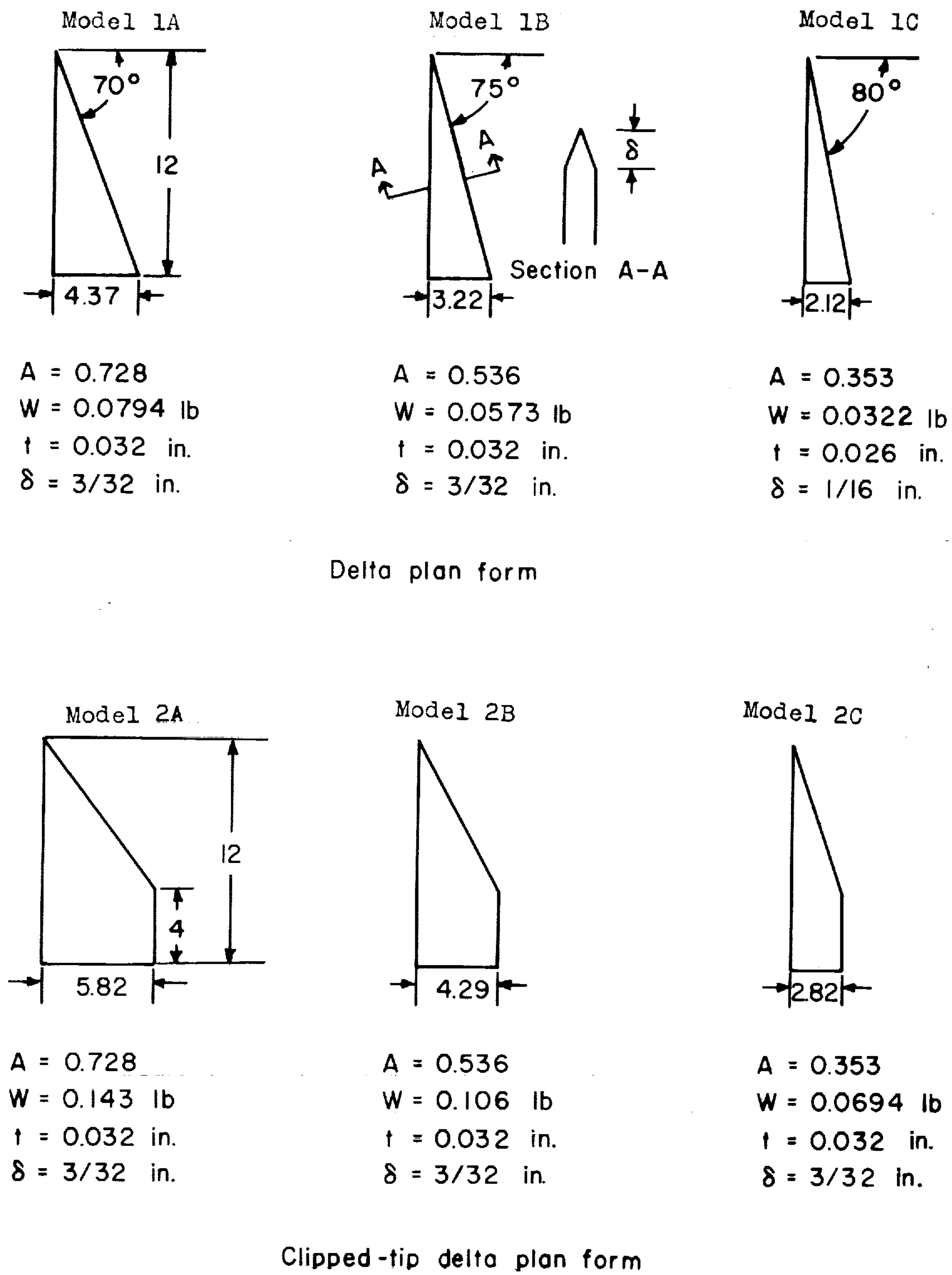

Figure 1.- Model geometry.

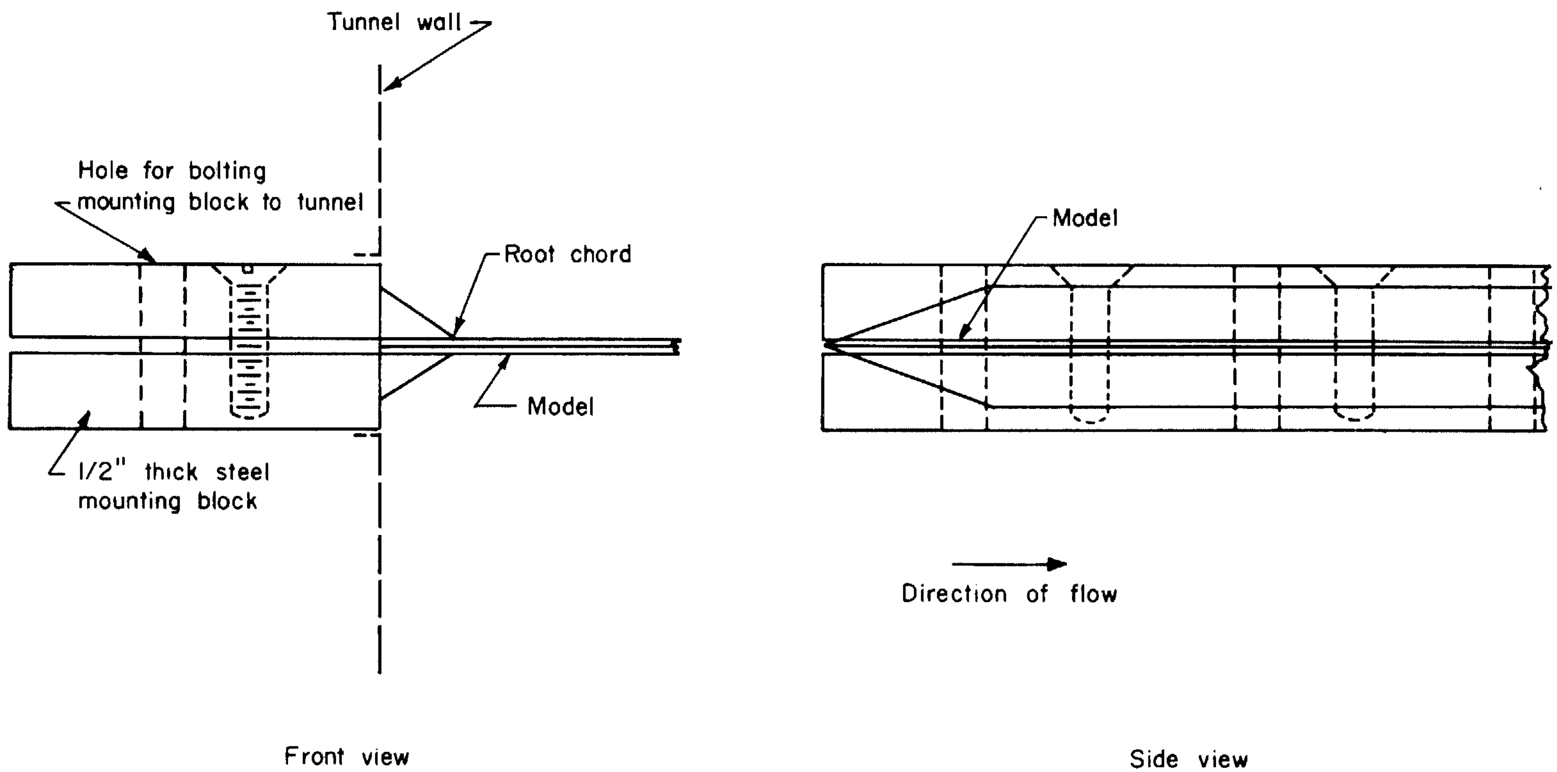

Figure 2.- Method of mounting models.

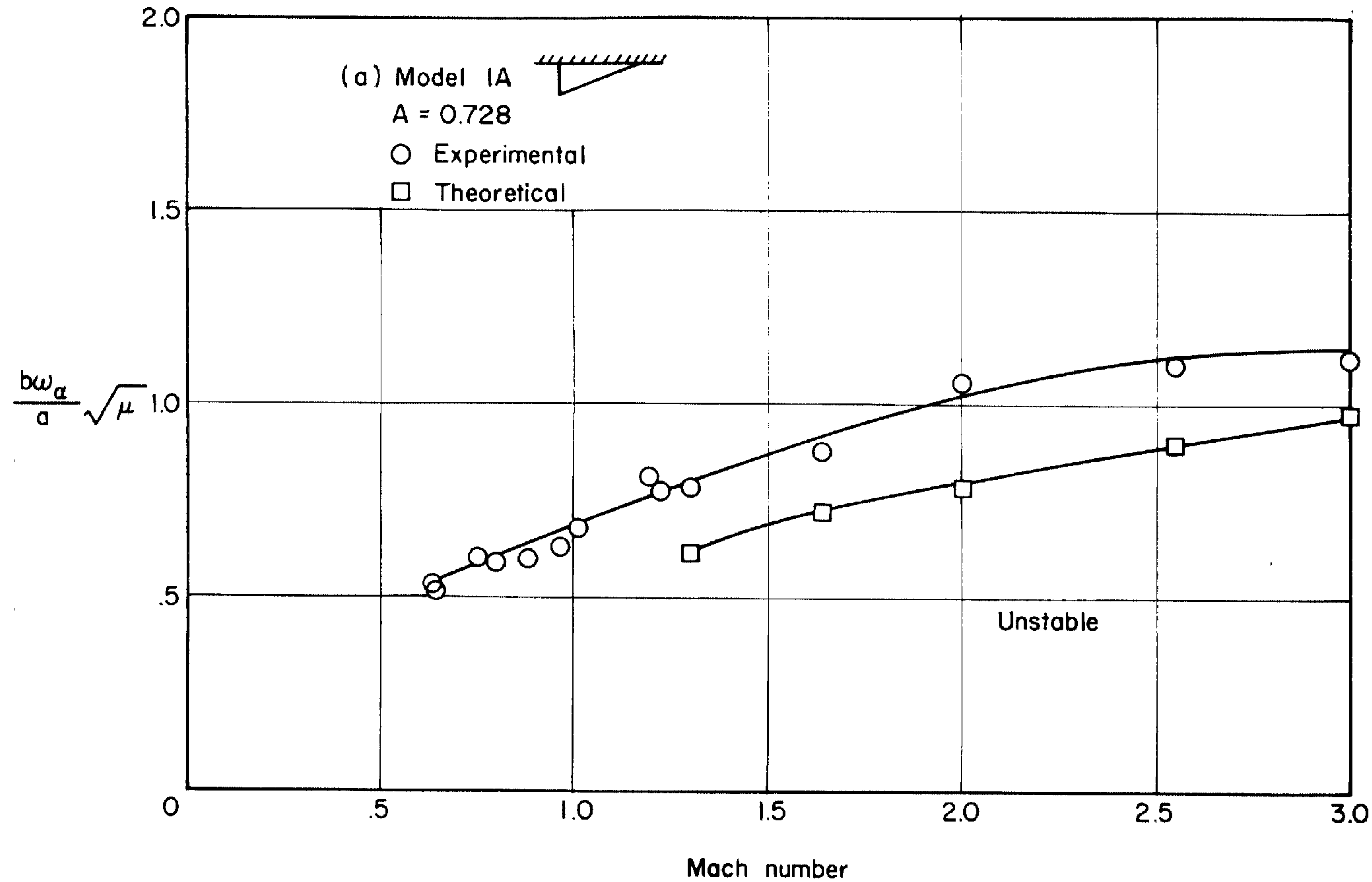

Figure 3.- Experimental and theoretical variation of stiffness-altitude parameter with Mach number.

L-256

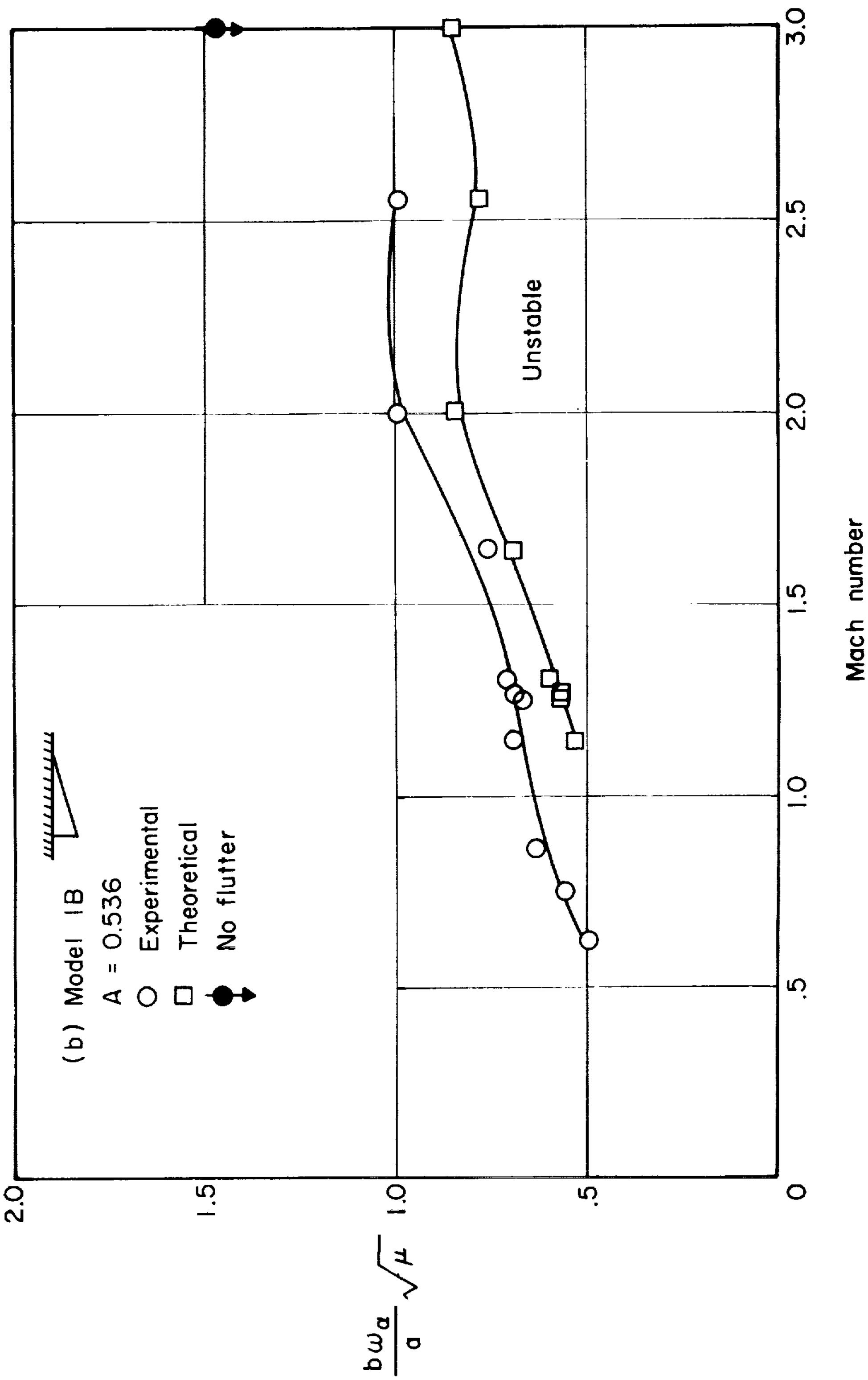

Figure 3.- Continued.

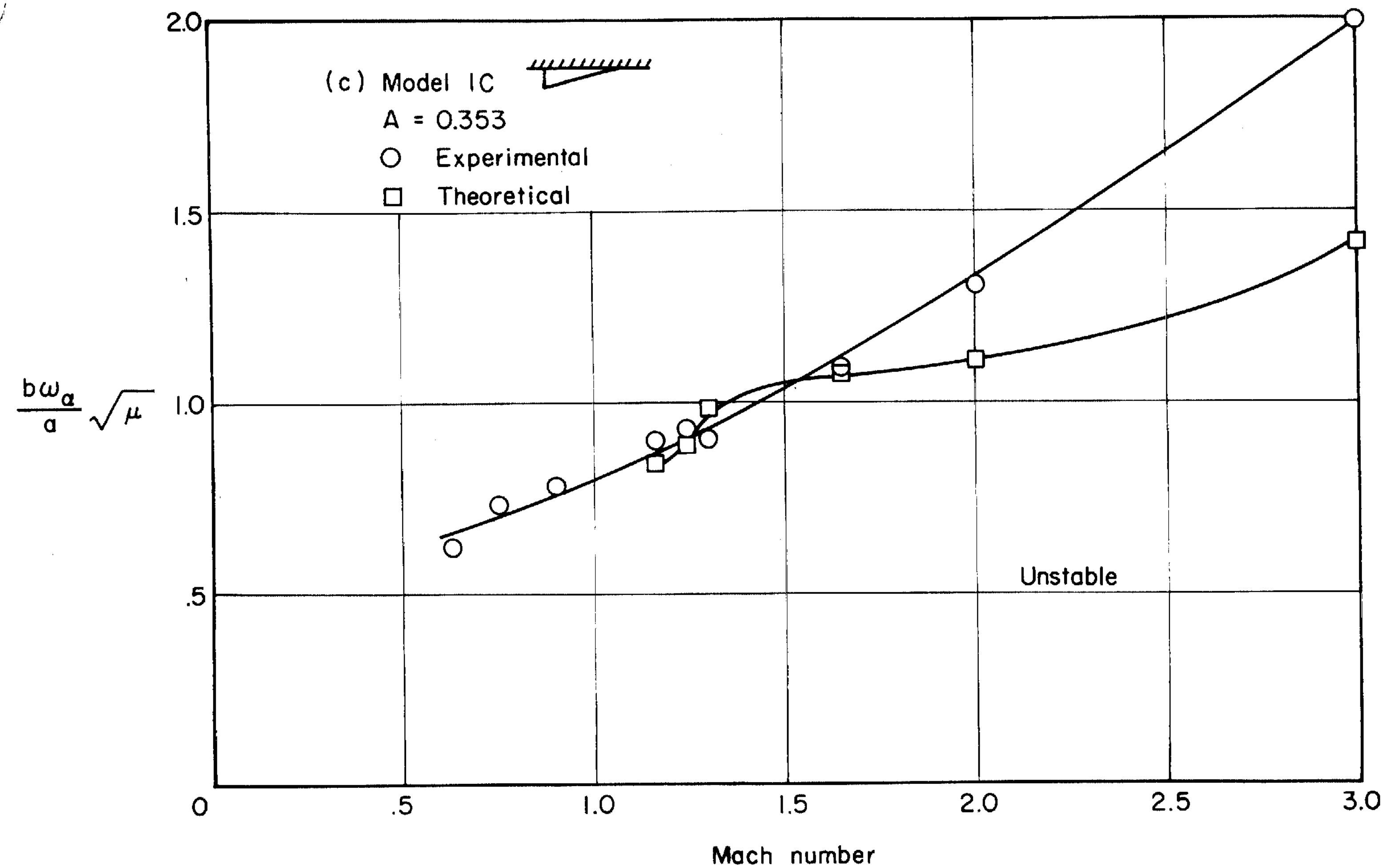

Figure 3.- Continued.

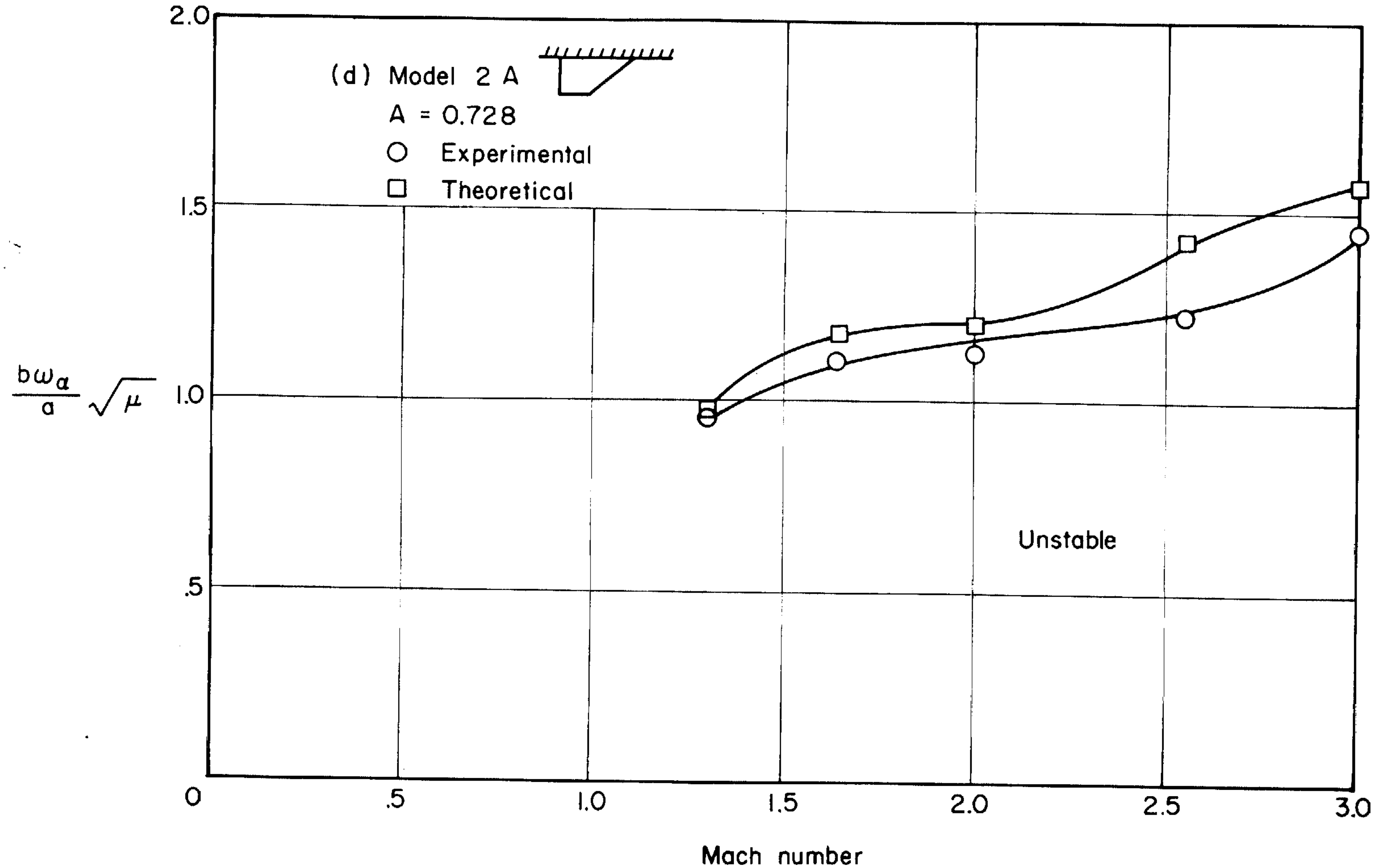

Figure 3.- Continued.

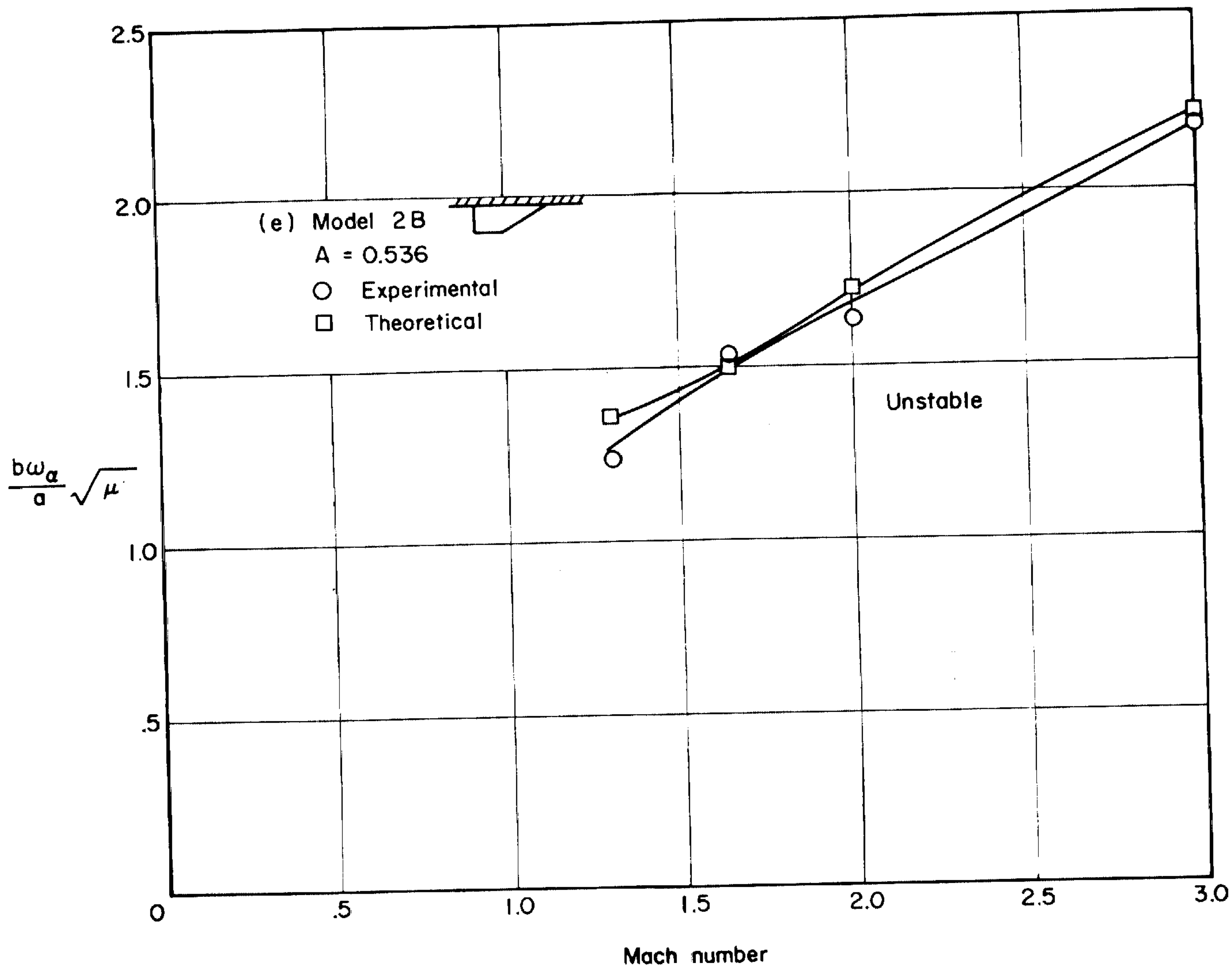

Figure 3.- Continued.

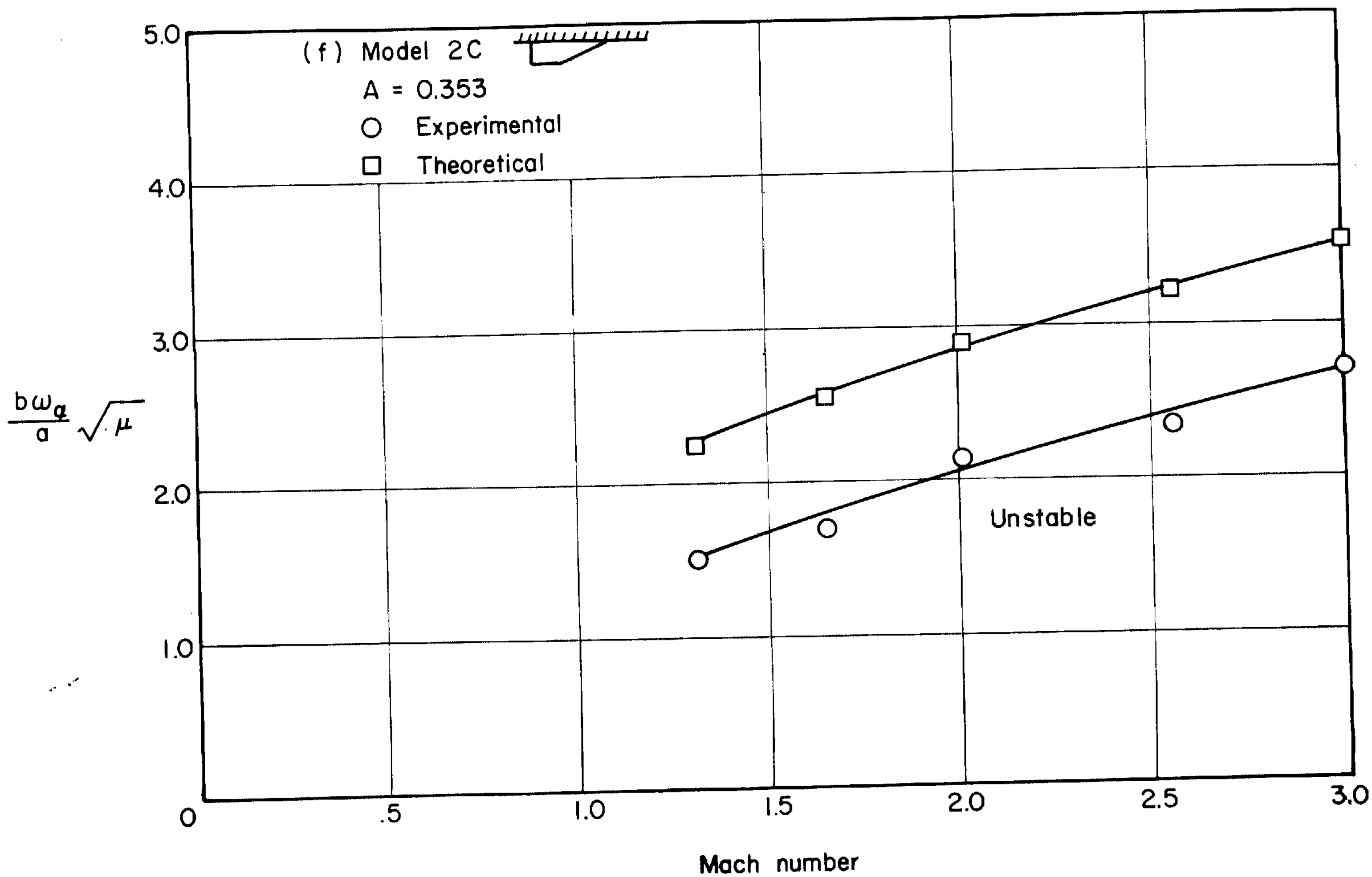

Figure 3.- Concluded.

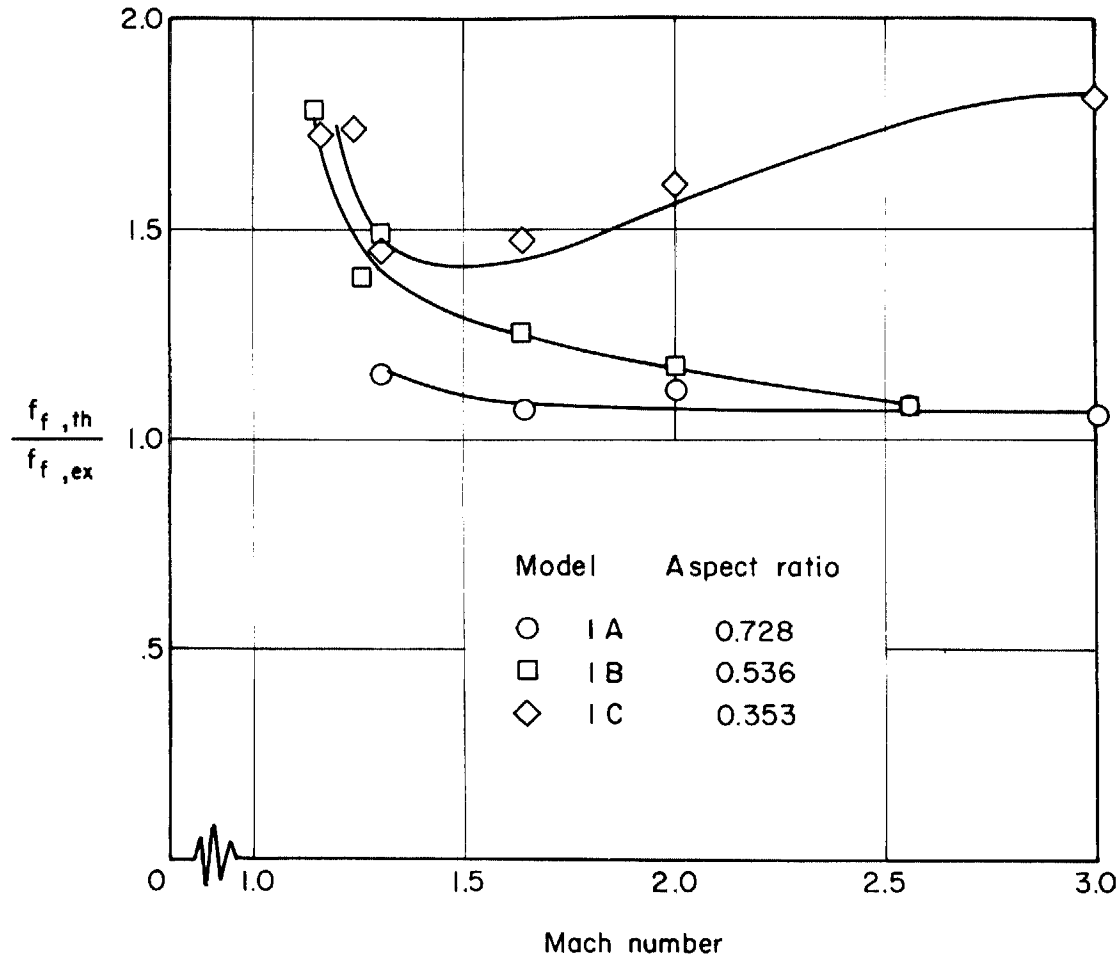

(a) Delta plan form.

Figure 4.- Variation of the ratio of theoretical to experimental flutter frequency with Mach number.

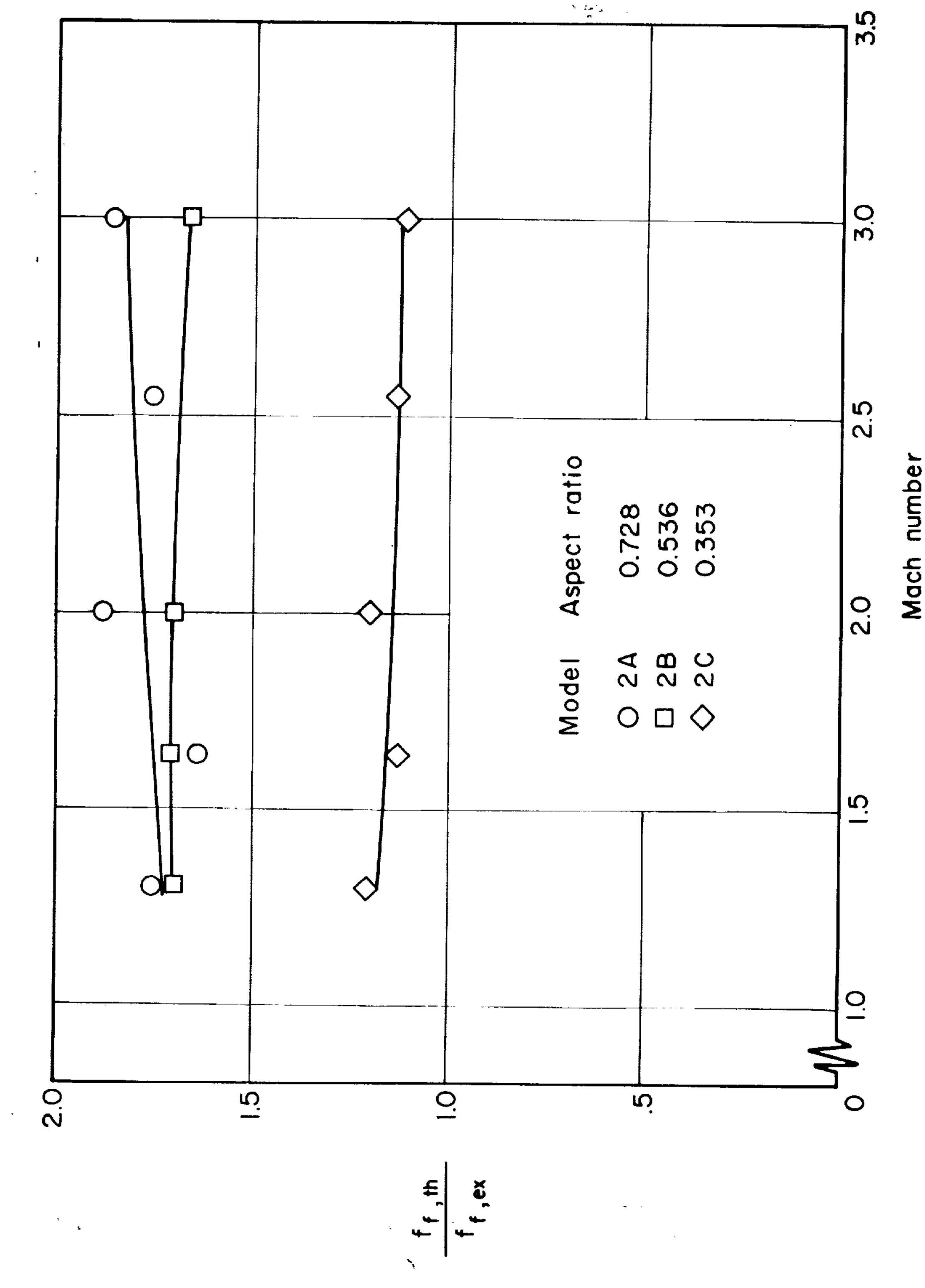

(b) Clipped-tip-delta plan form.

Figure 4.- Concluded.